CHEMICAL ENGINEERING TRANSACTIONS
VOL. 90, 2022
A publication of AIDIC
The Italian Association of Chemical Engineering
Online at www.cetjournal.it
Guest Editors: Aleš Bernatík, Bruno Fabiano

ISBN 978-88-95608-88-4; **ISSN** 2283-9216
DOI: 10.3303/CET2290090

Cryogenic Hydrogen Storage Tanks Exposed to Fires: a CFD Study

Federico Ustolin[a,*], Giordano E. Scarponi[b], Tommaso Iannaccone[b], Valerio Cozzani[b], Nicola Paltrinieri[a,b]

[a] Department of Mechanical and Industrial Engineering, Norwegian University of Science and Technology NTNU, Richard Birkelands vei 2B, 7034 Trondheim, Norway
[b] LISES - Dipartimento di Ingegneria Civile, Chimica, Ambientale e dei Materiali, Alma Mater Studiorum - Università di Bologna, via Terracini n.28, 40131 Bologna, Italy
federico.ustolin@ntnu.no

Hydrogen is one of the most suitable candidates in replacing heavy hydrocarbons. Liquefaction of fuels is one of the most effective processes to increase their low density. This is critical especially in large-scale or mobile applications such as in the maritime or aeronautical fields. A potential loss of integrity of the cryogenic storage equipment might lead to severe consequences due to the properties of these substances (e.g. high flammability). For this reason, this critical event must be avoided. The aim of this study is to analyse the behaviour of the cryogenic vessel and its lading when it is exposed to a fire and understand how to prevent a catastrophic rupture of the tank during this accident scenario.
A two-dimensional computational fluid dynamic (CFD) analysis is carried out on a cryogenic liquid hydrogen (LH_2) vessel to investigate its thermal response when engulfed in a fire. The model accounts for the evaporation and condensation of the substance and can predict the tank pressurization rate and temperature distribution. It is assumed that the vessel is completely engulfed in the fire (worst-case scenario). The CFD model is validated with the outcomes of a small-scale fire test of an LH_2 tank. Critical indications on the dynamic response of the cryogenic tank involved in a worst-case accident scenario are provided. Tank pressurisation and temperature distributions of the case study can be exploited to provide conservative estimations of the time to failure (TTF) of the vessel. These outcomes represent useful information to support the emergency response to this type of accident scenario and can aid the selection of appropriate and effective safety barriers to prevent the complete destruction of the tank.

1. Introduction

In the near future, the consumption of low- or zero-emission fuels might increase to reduce the environmental pollution, greenhouse gas emission and related issues such as global warming. Hydrogen is a zero-emission fuel if used in fuel cells, and it is potentially renewable if produced from water. Liquid hydrogen (LH_2) is one of the best options to store large amounts of hydrogen and tackle its low-density issue. LH_2 is stored close to atmospheric pressure in cryogenic conditions (20 K (NIST, 2019)) in double walled super insulated vessels. Gaseous hydrogen (GH_2) is always present in any LH_2 storage component due to the boil-off gas (BOG) formation caused by the heat losses with the surroundings. Therefore, the hazards related to GH_2 must be always considered when LH_2 is employed, beyond the cryogenic hazard represented by its ultra-low boiling point. Hydrogen is known to be extremely flammable and difficult to detect. For these reasons, a loss of containment (LOC) must be avoided. Beyond the fire that might result after the LOC of hydrogen equipment, a boiling liquid expanding vapour explosion (BLEVE) may be generated after the catastrophic rupture of a vessel containing a liquefied gas. BLEVE is an atypical accident scenario since it is not always considered as direct consequence of a complete destruction of the tank (Ustolin et al., 2020a). This phenomenon and all types of emerging risks must be prevented when hydrogen is deployed for new applications such as the maritime ones. In the past, few works analysed the atypical accident scenarios for LH_2 vessels. For instance, Scarponi et al.

Paper Received: 9 December 2021; Revised: 17 March 2022; Accepted: 1 May 2022
Please cite this article as: Ustolin F., Scarponi G.E., Iannaccone T., Cozzani V., Paltrinieri N., 2022, Cryogenic Hydrogen Storage Tanks Exposed to Fires: a CFD study, Chemical Engineering Transactions, 90, 535-540 DOI:10.3303/CET2290090

(2016) and Ustolin et al. (2021) developed a lumped model to estimate the pressure build-up inside the liquefied natural gas (LNG) and LH_2 tanks when exposed to a fire, respectively, while the consequences of an LH_2 were assessed in (Ustolin et al., 2020a) and the ones of methane and propane tanks in (Ustolin et al., 2020b).
This study focused on the modelling of an LH_2 tank exposed to a fire. The behaviour of the tank lading was investigated thanks to a CFD analysis. In particular, the tank pressure build-up and the temperature increase were simulated as well as the hydrogen evaporation-condensation. The CFD model developed in this study was then validated with an LH_2 tank fire test published by Pehr (1996). The aim of this paper is to provide a tool to characterize LH_2 tank behaviour under fire exposure so that measure can be put in place to prevent LOC. For instance, the CFD model can be employed to estimate the time to failure (TTF) of the LH_2 vessel and provide critical indications to the emergency responders. A similar model can be employed for other types of liquefied gases as already done for LNG in (Iannaccone et al., 2021) and liquefied petroleum gas (LPG) in (Scarponi et al., 2019).

2. Methodology

A 2D computational fluid dynamics (CFD) model was developed in Ansys Fluent® to study the behaviour of a cryogenic tank content when exposed to a fire. Particularly, the model developed by Scarponi et al. (2018) to analyse LPG tanks engulfed in fire end extended to LKG tanks by Iannaccone et al. (2021) was adapted for LH_2 tanks. The CFD simulation domain consisted of the cross-section of the cryogenic double walled tank horizontally oriented and composed by the inner and outer shells separated by a vacuum jacket where the insulation was installed. In this study, multilayer vacuum insulation (MLVI) was considered as thermal protection of the vessel. The governing equations for the turbulent, two phases, transient CFD setup implemented in Fluent can be found in (Iannaccone et al., 2021). The tank lading was composed by both LH_2 and GH_2. Due to the extremely low temperature of LH_2 (-253 °C (NIST, 2019)), para-hydrogen was chosen instead of normal-hydrogen. The properties of the fluid such as density, specific heat capacity, viscosity and thermal conductivity were gathered from the NIST database (NIST, 2019) where the Helmholtz Free Energy equation of state is employed (Leachman et al., 2009). The properties were implemented in Fluent as piece-wise linear function of temperature. The Peng Robinson equation of state was selected to estimate the density of the gaseous phase. The density of the MLVI insulation was taken from Barron and Nellis (2016) by considering its layer density, while thermal conductivity of the MLVI was estimated by following the procedure suggested in the ISO21013-3:2016 standard (ISO, 2016). The MLVI specific heat capacity at constant pressure (c_p) was calculated with the rule of mixture (Eq.(1)) as suggested by Motes and Hegeman (2019).

$$c_{p,MLVI} = x_1 c_{p,1} + x_2 c_{p,2} + \cdots + x_t c_{p,t} \quad (1)$$

where c_p are the specific heat capacities of the species which compose the MLVI (e.g. metals, polymers) in J kg^{-1} K^{-1}, and x is the fraction of each species. A similar procedure to estimate the MLVI properties was adopted in (Ustolin et al., 2021).

2.1 Numerical settings

The volume of fluid (VOF) multiphase model was selected to solve the continuity equation. The evaporation-condensation model implemented in Fluent (Lee, 1979) was employed to estimate the mass transfer between the liquid and gaseous phases. The default value of 0.1 was kept for the evaporation-condensation frequency coefficients. The k-ω shear stress transport (SST) turbulence model was selected to simulate the turbulent natural convection regime. The semi-implicit method for pressure linked equations-consistent (SIMPLEC) algorithm was selected for the pressure-velocity coupling. The transient analysis was modelled by means of the first-order implicit scheme, considering a time step of 0.01 s. Second-order discretization schemes were adopted for density, momentum, energy, turbulent kinetic energy (k) and dissipation rate (ω). The pressure staggering option (PRESTO!) and geo-reconstruction schemes were used for pressure and volume fraction, respectively. The gradients are discretized with the least square cell-based equation. The under-relaxation factors set in the analysis are collected in Table 1.

Table 1: Values of selected under-relaxation factors

	Pressure	Density	Body forces	Momentum	Vaporization mass	k and ω	Energy	Other variables
Value	0.3	0.7	0.7	0.5	0.7	0.8	0.8	1.0

2.2 BMW fire test case study

The fire test reported in (Pehr, 1996) was simulated in this study. During the experiment, the double walled LH_2 tank described in (Rüdiger, 1992) was tested. This LH_2 vessel had a volume of 0.122 m^3 and was thermally protected with 80 layers of multilayer insulation (MLI) installed together with two vapour-cooled radiation shields in a 35 mm gap between the inner and outer shells (Rüdiger, 1992). Since the vacuum is created in this interstice, this type of insulation is defined as multilayer vacuum insulation (MLVI). The LH_2 vessel was horizontally oriented and completely engulfed in a propane fire during the experiment. The average temperature of the flames was 920 °C (Pehr, 1996). Almost half of the tank (55%) was filled with LH_2. Two pressure relief valves (PRVs) installed on the tank were placed outside the fire area to avoid any opening induced by heat leakage. The pressure in the vacuum cavity increased due to the thermal decomposition of the MLVI materials during the fire test. This led to an increase of the insulation thermal conductivity with a consequent tank pressure build-up. The PRVs were activated for the first time when the tank reached a pressure of 4.6 bar, approximately six minutes after the ignition of the propane fire. The whole tank lading was fully vented 14 minutes after the beginning of the test. The outer shell made of austenitic steel resisted to the fire for more than one hour. Contrarily, the inner aluminium tank melted when emptied. Despite this is a unique and critical test, the description of few parameters was not published. In particular, the materials of the MLVI insulation were not specified, thus their properties such as density, thermal conductivity and c_p must be assumed. The broad temperature gradients generated within the tank due to the different properties of the hydrogen phases cannot be investigated due to the unknown positions of the temperature sensors. Moreover, the size (diameter) of the PRVs was not reported. Furthermore, the temperature measurements published in (Pehr, 1996) are all depicted on the same graph (temperature range of 1,400 K) making difficult to read and extrapolate the data. Regarding the tank dimensions, only the internal volume and the insulation thickness were specified by Rüdiger (1992). Therefore, it was assumed that the internal diameter of the inner tank was 460 mm, and the tank walls thickness was 3 mm. The characteristics of the simulated tank are summarised in Table 2.

Table 2: Characteristics of the simulated tank (abbreviation: MLVI: multilayer vacuum insulation)

	Tank volume (m^3)	Tank internal diameter (m)	Type of insulation	Insulation thickness (m)	Tank wall thickness (m)
Value	0.122	0.460	MLVI	0.035	0.003

A grid independence study was carried out. The computational mesh was unstructured, i.e. composed by both quadrilateral and triangular elements. The maximum cell size was 3 mm with a global growth rate of 1.1. The walls of the inner and the outer shells were divided in 241 segments. In this way, the length of each of these segments was approx. 3 mm. A total of 25 inflation layers with a first layer thickness of 0.2 mm were implemented on the inner tank wall with a growth rate of 1.2 toward the centre of the vessel in order to increase the grid resolution in the near wall region. The symmetry condition was imposed along the transversal axis of the tank in order to reduce the number of cells in the grid, thus the computational time. The total number of cells was 17,029. The initial conditions for the simulation were set in accordance with the experimental ones (Pehr, 1996). The temperatures of the liquid phase was set equal to 20 K, while a linear vertical temperature gradient between 20 and 36 K was imposed in the gaseous phases by means of a user define function (UDF). The filling degree of the tank was 55% which corresponds to a height of the liquid-vapor interface of 253 mm for this tank size. The initial tank pressure was slightly above the atmospheric one (160 kPa). An external radiation temperature of 920 °C (~ 1,193 K) was selected on the outer tank wall for the radiation thermal condition as boundary condition to simulate the propane fire. A total of four case studies was defined. In case studies A, B and C three different constant values for the MLVI thermal conductivity were considered. In case D, with the aim of mimicking the effect of the loss of vacuum and MLVI materials degradation caused by the fire exposure, a time varying value was assumed for this parameter. The value of the MLVI thermal conductivity was calculated with the abovementioned ISO standard by considering that each layer of the insulation was made of a 0.006 mm aluminium foil and a 0.015 mm fiberglass paper with a degree of vacuum of 13.3 mPa. On the other hand, this property was also estimated in case of a complete loss of vacuum and penetration of hydrogen inside the insulation. In the case D, the MLVI thermal conductivity was changed at 115 s. This time was deducted by observing the experimental pressure and temperature curves, that show a sudden increase of tank pressure and temperatures starting from 115 s. Finally, the PRVs installed on the tank were neglected making not possible to reproduce the entire experiment. Hence, the total simulation time was 351 s, i.e. when the PRVs opened for the first time.

The MLVI density was 167 kg m^{-3}, estimated for a layer density of 23 layers cm^{-1}. The calculated c_p of the MLVI insulation was 881.5 J kg^{-1} K^{-1}. The estimated MLVI thermal conductivities before and after the loss of vacuum

were 1.5 and 239.0 mW m^{-1} K^{-1}, respectively. However, the simulated pressure build-up and temperatures did not match the experimental outcomes if these values were set in the simulations. Therefore, the thermal conductivity was changed to 160.0 mW m^{-1} K^{-1} for the case C. Since the model results were too conservative, the thermal conductivity was changed from 1.5 to 160.0 mW m^{-1} K^{-1} through a UDF in Fluent at the simulated time of 115 s (case D). The MLVI properties for the four case studies are listed in Table 3.

Table 3: MLVI calculated properties

	Density (kg m^{-3})	c_p (J kg^{-1} K^{-1})	Thermal conductivity (mW m^{-1} K^{-1})			
			Case A	Case B	Case C	Case D
Value	167.0	881.5	1.5	239.0	160.0	1.5 0 ≤ t ≤ 115 s 160.0 t > 115 s

3. Results and discussion

The first three case studies could not match the experimental results (Figure 1a). In fact, case A underestimated the pressure build-up, while case B and C overestimated it. On the other hand, a good agreement was shown between the last simulation (case D) and the experimental outcomes in regards of pressure and temperatures as can be noticed in Figure 1. For this reason, the following discussion focuses on the outcomes of case D only. The tank pressure was slightly conservative at the end of the simulation (Figure 1a) as well as the minimum LH_2 temperature, while the maximum GH_2 one was underestimated (Figure 1b). As previously mentioned, the positions of the thermocouples within the tank are unknown. Therefore, it is not clear if the measured GH_2 temperature is the highest one within the tank. Furthermore, the simulated LH_2 temperature is largely higher than the measured one since the latter remained constant at 20 K until the whole tank content evaporated. Thus, a large relative error of 33% was committed. It might be possible that small temperature variations cannot be spotted on the chart published by Pehr (1996) due to the vast temperature range (1,400 K) on the axis as described above. Hence, it is unclear if the large error is caused by the unprecise reading of the chart or by the CFD code and hydrogen properties setting. It might be possible that the hydrogen properties influenced the accuracy of the CFD outcomes since these are barely temperature dependent. This means that only the hydrogen saturation properties were implemented in this model for both LH_2 and GH_2 phases.

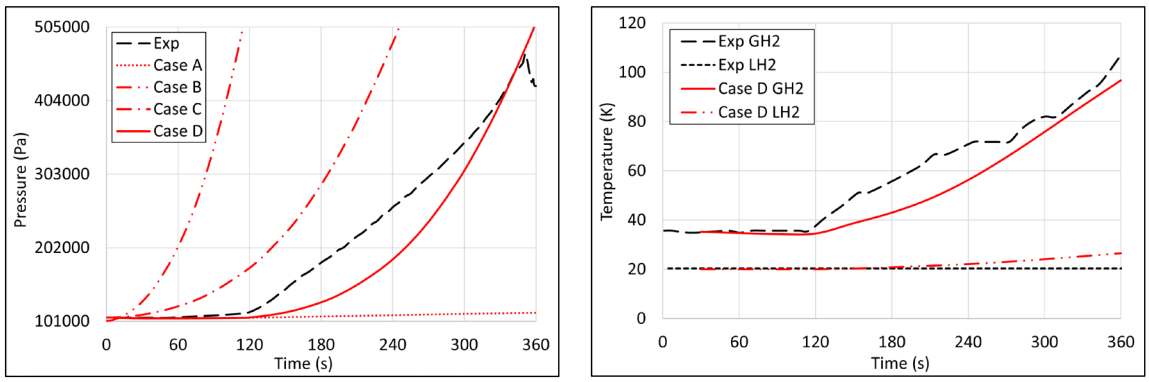

Figure 1: Comparison between the (a) pressures and (b) lowest LH_2 and highest GH_2 temperatures estimated by the CFD analysis for the different case studies (red lines) and measured during the experiment (black lines)

The temperature gradient and the stratification within the inner tank simulated by the CFD code can be appreciated in Figure 2a. As expected, a wide temperature gradient can be found in the gaseous phase (70 K), while only a 2 K temperature range was assessed in the liquid phase. Another issue related to the LH_2 is represented by the LH_2 level. During the fire test, the liquid level sensor measured an almost constant filling degree of 55-56% until the hydrogen venting started through the PRVs. On the opposite, the liquid level in the CFD simulation increased due to the increase in LH_2 temperature with the consequent drop of its density. Therefore, the CFD code estimated a liquid level of 270 mm at the end of the simulation (Figure 2b) which corresponds to a filling degree of 60%. In Table 5, the simulated tank pressure, temperatures and filling degree in the case D are compared with the measured ones at 351 s. The relative errors are also reported in Table 4.

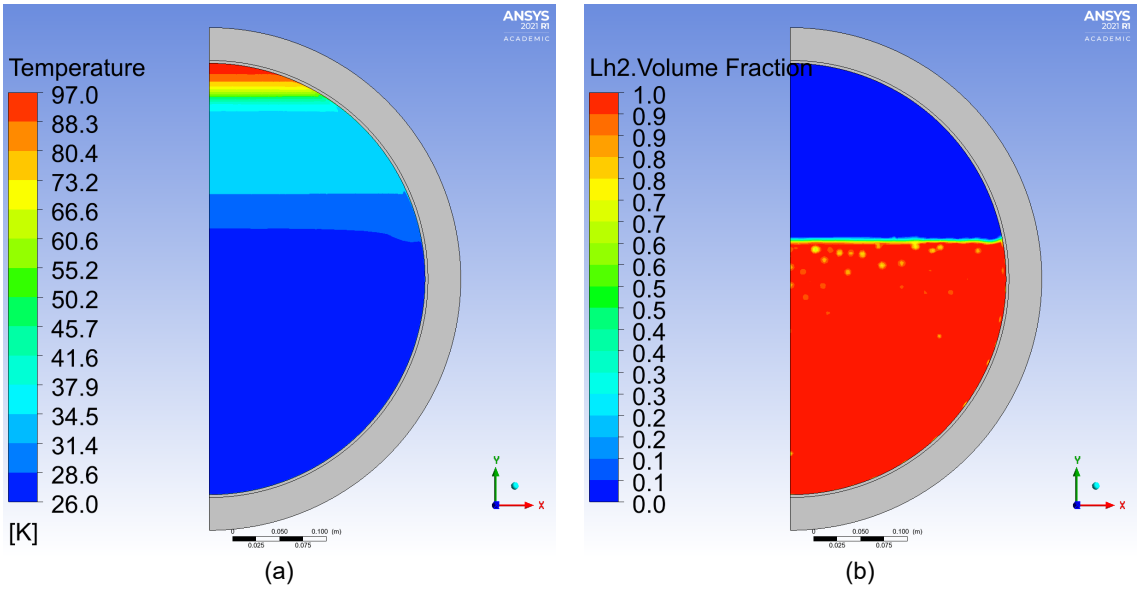

Figure 2: CFD contours of the (a) temperature gradients and (b) liquid hydrogen volume fraction in the inner tank at the end of the case D simulation (351 s)

Table 4: Comparison between simulated (case D) and measured values of pressure, temperatures, and filling degree at 351 s

	Pressure (Pa)	Pressure error (%)	GH_2 temp (K)	GH_2 temp error (%)	LH_2 temp (K)	LH_2 temp error (%)	Filling degree (%)	Filling degree error (%)
Experiment	467,800	-	107.0	-	20.0	-	56	-
CFD	476,247	1.8	96.7	9.6	26.6	33.0	60	7.1

As shown in Figure 1, the MLVI properties (in particular the thermal conductivity), which are unknown for the considered fire test, have a strong influence on the model results. Pehr (1996) demonstrated that the MLVI changed its properties during the experiment due to the fire exposure with consequent vacuum loss and material degradation. Additional tests on the fire resistance of the insulation materials are required to better assess the modification of insulation characteristics. The evaporation-condensation frequency coefficients of the Lee model might be modified in future studies to better estimate the maximum hydrogen temperature which was underestimated in case D. Further experiments on the evaporation of para-hydrogen are suggested to define the most accurate values of these coefficients, or suggest the employment of different evaporation-condensation model. Moreover, the CFD model can be refined and improved by implementing in Fluent the hydrogen thermodynamic properties dependent on both temperature and pressure from the NIST database by means of a UDF. Nevertheless, the presented model can satisfactorily assess the pressure build-up in the LH_2 tank and be exploited to determine the time to failure of the vessel. Finally, the fire test analysed in this work is the only one carried out on double walled LH_2 tanks according to the authors' knowledge. The heat transfer and the pressure build-up strongly depend on the surface to volume ratio of the vessel. This means that a different behaviour would manifest for larger container. Therefore, additional fire tests on this type of vessels are suggested. This is one of the objectives of the safe hydrogen fuel handling and use for efficient implementation (SH_2IFT) project in which fire tests will be conducted on different double walled LH_2 tanks with a volume of 1 m^3 (Sintef, 2019). The aim of these tests is to assess the tank performance under fire conditions and characterize the risk of explosion.

4. Conclusions

This study highlighted the effect of fire exposure on a cryogenic hydrogen vessel. The behaviour of the tank lading during a fire test was simulated and analysed by means of a CFD analysis. The developed model was validated with experimental data and, considering the uncertainties on experimental measurements and specification, a reasonable agreement was found. Additional experiments are necessary to investigate the behaviour of this type of vessels and their lading during this type of accident scenario, determine the vessel TTF

and further validate the proposed model. Finally, this numerical approach can aid and support the risk assessment and emergency response planning of cryogenic liquefied gas vessels.

Acknowledgments

This work was undertaken as part of the research project Safe Hydrogen Fuel Handling and Use for Efficient Implementation (SH_2IFT), and the authors would like to acknowledge the financial support of the Research Council of Norway under the ENERGIX programme (Grant No. 280964).

References

Barron R.F., Nellis G.F. (Eds.), 2016, Cryogenic Heat Transfer, CRC Press, Boca Raton, Florida.

Iannaccone T., Scarponi G.E., Landucci G., Cozzani V., 2021, Numerical simulation of LNG tanks exposed to fire. Process Safety and Environmental Protection, 149, 735–749.

ISO, 2016, Cryogenic vessels — Pressure-relief accessories for cryogenic service — Part 3: Sizing and capacity determination — ISO21013-3:2016.

Leachman J.W., Jacobsen R.T., Penoncello S.G., Lemmon E.W., 2009, Fundamental Equations of State for Parahydrogen, Normal Hydrogen, and Orthohydrogen, Journal of Physical and Chemical Reference Data, 38, 721–748.

Lee W.H., 1979, A Pressure Iteration Scheme for Two-Phase Modeling, Tech. Rep.LA-UR, Los Alamos Sci. Lab. Los Alamos, New Mex, 79–975.

Motes D., Hegeman T., 2019, Means to Determine Heat Capacities of Multilayer Insulation Materials, DSIAC-2019-1156, Department of Defense Information Analysis Center.

NIST, 2019, NIST Chemistry WebBook 69, National Institute of Standards and Technology <webbook.nist.gov/chemistry/> accessed 19.03.2019.

Pehr K., 1996, Experimental examinations on the worst-case behaviour of LH2/LNG tanks for passenger cars, Proceedings of the 11th World Hydrogen Energy Conference, 2169–2187.

Rüdiger H., 1992, Design characteristics and performance of a liquid hydrogen tank system for motor cars, Cryogenics, 32, 327–329.

Scarponi G.E., Landucci G., Ovidi F., Cozzani V., 2016, Lumped Model for the Assessment of the Thermal and Mechanical Response of LNG Tanks Exposed to Fire, Chemical Engineering Transaction, 53, 307–312.

Scarponi G.E., Landucci G., Birk A.M., Cozzani V., 2018, LPG vessels exposed to fire: Scale effects on pressure build-up, Journal of Loss Prevention in the Process Industries, 56, 342–358.

Scarponi G.E., Landucci G., Birk A.M., Cozzani V., 2019, An innovative three-dimensional approach for the simulation of pressure vessels exposed to fire, Journal of Loss Prevention in the Process Industries, 61, 160–173.

Sintef, 2019, SH_2IFT - Safe Hydrogen Fuel Handling and Use for Efficient Implementation <sintef.no/projectweb/sh2ift/> accessed 02.09.2019.

Ustolin F., Paltrinieri N., Landucci G., 2020a, An innovative and comprehensive approach for the consequence analysis of liquid hydrogen vessel explosions, Journal of Loss Prevention in the Process Industries, 68, 104323.

Ustolin F., Salzano E., Landucci G., Paltrinieri N., 2020b, Modelling Liquid Hydrogen BLEVEs: A Comparative Assessment with Hydrocarbon Fuels, Proceedings of the 30th European Safety and Reliability Conference and 15th Probabilistic Safety Assessment and Management Conference (ESREL2020 PSAM15).

Ustolin F., Iannaccone T., Cozzani V., Jafarzadeh S., Paltrinieri N., 2021, Time to Failure Estimation of Cryogenic Liquefied Tanks Exposed to a Fire, Proceedings of the 31st European Safety and Reliability Conference, 935–942.